PHYSICAL REVIEW D **79,** 095014 (2009)

LHC discovery potential of a leptophilic Higgs boson

Shufang Su* and Brooks Thomas†

Department of Physics, University of Arizona, Tucson, Arizona 85721, USA

(Received 27 March 2009; published 20 May 2009)

In this work, we examine a two-Higgs-doublet extension of the standard model in which one Higgs doublet is responsible for giving mass to both up- and down-type quarks, while a separate doublet is responsible for giving mass to leptons. We examine both the theoretical and experimental constraints on the model and show that large regions of parameter space are allowed by these constraints in which the effective couplings between the lightest neutral Higgs scalar and the standard-model leptons are substantially enhanced. We investigate the collider phenomenology of such a ''leptophilic'' two-Higgs-doublet model and show that in cases where the low-energy spectrum contains only one light, *CP*-even scalar, a variety of collider processes essentially irrelevant for the discovery of a standard model Higgs boson (specifically those in which the Higgs boson decays directly into a charged-lepton pair) can contribute significantly to the discovery potential of a light-to-intermediate-mass ($m_h \lesssim 140$ GeV) Higgs boson at the LHC.

DOI: 10.1103/PhysRevD.79.095014 PACS numbers: 14.80.Cp

I. INTRODUCTION

One of the primary goals of the Large Hadron Collider (LHC), a proton-proton collider with a center of mass energy $\sqrt{s} = 14$ TeV, will be to investigate the sector responsible for the breaking of the electroweak symmetry. In the standard model (SM), a single Higgs doublet is responsible for the spontaneous breakdown of the $SU(2)_L \times U(1)_Y$ gauge group to $U(1)_{\mathrm{EM}}$. The coupling constants of the sole physical Higgs scalar to the rest of the SM particles are completely determined by their masses, and consequently there is little guesswork involved in determining the most promising channels [1,2] in which one might hope to discover such a scalar. For a relatively light ($114\ \mathrm{GeV} \lesssim m_h \lesssim 125\ \mathrm{GeV}$) SM Higgs boson, those channels are $gg \to h \to \gamma\gamma$ and $t\bar{t}h(h \to b\bar{b})$, while for an intermediate-mass ($125\ \mathrm{GeV} \lesssim m_h \lesssim 140\ \mathrm{GeV}$) Higgs, the single most promising channel is the weak-boson fusion (WBF) [3] process $qq' \to qq'h(h \to \tau\tau)$ [4]. For a heavier Higgs, with $m_h \gtrsim 140$ GeV, the most relevant channels are $h \to WW^*$ and $h \to ZZ^*$, with the Higgs produced via either gluon fusion or WBF [1,2].

In models where the Higgs sector differs significantly from that of the standard model, however, the situation can change dramatically. This is true even in cases where the low-energy effective theory describing a given model at the weak scale contains only a single, light, *CP*-even Higgs scalar. Indeed, at low energies, many models with extended Higgs sectors have effective descriptions that are ''-standard-model-like'' in the sense that they contain a single light Higgs boson, but one whose couplings to the standard model fermions and gauge bosons differ—potentially significantly—from those of a SM Higgs. Such discrepancies, in turn, can translate into vast differences in LHC phenomenology: some (or, in severe cases, even all) of the standard detection channels for a SM Higgs may disappear as a result of such modifications, while others, related to processes buried beneath background in the SM, may become crucial for discovery.

One set of channels which are not terribly significant for the discovery of a SM Higgs, but could become so in models with modified Higgs sectors, consists of those involving direct decays of the Higgs boson to a pair of high-p_T leptons. In the SM, a light Higgs boson (with mass $m_h < 130$ GeV) decays predominantly into $b\bar{b}$, and the ratio $\mathrm{BR}(h \to \ell\ell)/\mathrm{BR}(h \to b\bar{b})$ (where $\ell = e,\ \mu,\ \tau$) is roughly proportional to m_ℓ^2/m_b^2, due to the fact that in the SM, the same Higgs doublet is responsible for giving mass to both quarks and leptons. Consequently, attention has been focused predominately on processes in which the Higgs boson decays to a tau pair (with a branching ratio of about 10%), and, in particular, on the weak-boson fusion process $qq' \to qq'h(h \to \tau\tau)$. This is the only process particularly relevant for SM Higgs discovery in which the Higgs decays directly to leptons, though it is now regarded as one of the most promising discovery channels for a SM Higgs in the intermediate mass region [3,5,6]. Searching for the Higgs in the $gg \to h \to \tau\tau$ and $tth(h \to \tau\tau)$ channels is more difficult, due to a combination of factors, including enhanced SM backgrounds and suppressed signal cross sections.

By contrast, processes in which a SM Higgs boson decays into first- or second-generation leptons are generally assumed to be irrelevant for discovery. This is because under the assumption of Yukawa-coupling universality among the lepton generations (an assumption we will be making throughout the present work), the small size of m_μ compared to m_τ results in $\mathrm{BR}(h \to \mu\mu)$ being roughly 2 orders of magnitude smaller than $\mathrm{BR}(h \to \tau\tau)$, with

*shufang@physics.arizona.edu
†brooks@physics.arizona.edu

 © 2009 The American Physical Society

BR($h \to ee$) nearly 3 orders of magnitude smaller still. Consequently, the rates for processes involving $h \to \mu\mu$ and $h \to ee$ are extremely suppressed relative to those involving tau pairs, both in the SM and in most simple extensions of the Higgs sector. On the other hand, there are strong motivations for considering processes of this sort at the LHC. Experimentally, a signal involving a pair of high-p_T muons or electrons will be easy to identify, as the muon- and electron-identification efficiencies at each of the LHC detectors are each greater than 90% [5,6]. Furthermore, once a Higgs boson is discovered in these channels, its mass could be readily reconstructed with high precision. Such channels could also be of use in determining the Higgs Yukawa couplings to leptons.

Two-Higgs-doublet models (2HDM), which stand as perhaps the simplest, most tractable example of a nonminimal electroweak-symmetry-breaking sector, provide a useful context in which to study the role of leptonic Higgs-decay processes. These models arise in a number of beyond-the-standard-model contexts from supersymmetry to little Higgs scenarios [7] and have a rich phenomenology, many of whose consequences for LHC physics are still being uncovered. In general, 2HDM can be categorized according to how the Higgs doublets couple to the SM quarks and leptons. In what has become known as a type I 2HDM, one doublet is responsible for the masses of both quarks and leptons, while the other decouples from the fermions entirely. In a type II 2HDM, one Higgs doublet couples to the up-type quark sector, while the other Higgs doublet couples to both the down-type quark sector and the charged leptons—as is the case, for example, in the minimal supersymmetric standard model (MSSM). In both of these standard scenarios, the leptonic branching ratios for a light Higgs do not differ much from their SM values throughout most of parameter space,[1] since the same doublet gives masses to both the bottom quark and the charged leptons.

One interesting alternative possibility, which will be the primary focus of the present work, is a 2HDM scenario in which one Higgs doublet couples exclusively to (both up- and down-type) quarks, while the other couples exclusively to leptons—a scenario which we will henceforth dub the leptophilic two-Higgs-doublet model (L2HDM).[2] This model has been discussed previously in the literature in relation to its effect on Higgs branching fractions and decay widths [9,11–13], flavor physics [14], and potential implications for neutrino phenomenology [15] and dark matter studies [10]. Some analyses of the LHC phenomenology of the model were presented in Ref. [10], which focused on the nondecoupling region of the parameter space where additional physical Higgs scalars are light.

In this work, we discuss the leptonic decays of the lightest CP-even Higgs scalar in the L2HDM at the LHC. In particular, we examine the discovery potential in a decoupling regime in which only one light scalar, which resembles the SM Higgs, appears in the low-energy effective description of the model. We begin in Sec. II by presenting the model and reviewing how the coupling structure of the lightest neutral Higgs particle is modified from that of a SM Higgs. In Sec. III, we discuss the applicable experimental constraints from flavor physics, direct searches, etc. and show that they still permit substantial deviations in the couplings between the Higgs boson and the other SM fields away from their standard-model values. In Sec. IV, we discuss the implications of such modifications on the Higgs branching ratios and production rates. In Sec. V, we discuss potential Higgs discovery channels in which the Higgs boson decays directly into a pair of charged leptons, and in Sec. VI, we calculate the discovery potential for a light, leptophilic Higgs using the combined results from all of these leptonic channels. In Sec. VII we conclude.

II. THE LEPTOPHILIC 2HDM

The L2HDM, as defined here, is a modification of the SM in which the Higgs sector consists of two $SU(2)_L \times U(1)_Y$ scalar doublets, both of which receive nonzero vacuum expectation values. The first of these doublets, which we call ϕ_q, couples only to (both up- and down-type) quarks, while the other, which we call ϕ_ℓ, couples only to leptons. In other words, the Yukawa interaction Lagrangian is specified to be

$$\begin{aligned}\mathcal{L}_{\text{Yukawa}} = &-(y_u)_{ij}\bar{q}_i\phi_q^c u_j - (y_d)_{ij}\bar{q}_i\phi_q d_j \\ &- (y_e)_{ij}\bar{\ell}_i\phi_\ell e_j + \text{H.c.},\end{aligned} \tag{1}$$

where $(y_u)_{ij}$, $(y_d)_{ij}$, and $(y_e)_{ij}$ are 3×3 Yukawa matrixes, q_i and ℓ_i respectively denote the left-handed quark and lepton fields, u_i and d_i respectively denote the right-handed up- and down-type quark fields, and e_i denotes the right-handed lepton fields. This coupling structure can be achieved by imposing a $\mathbb{Z}_2$ symmetry under which ϕ_ℓ and e_i are odd, while all the other fields in the model are even. We will assume that this symmetry is broken only softly, by a term of the form $(m_{q\ell}^2\phi_q^\dagger\phi_\ell + \text{H.c.})$ in the scalar potential.

In the L2HDM, that scalar potential takes the usual form common to all two-Higgs doublet models. Assuming that there is no CP-violation in the Higgs sector, this potential can be parametrized as follows [16]:

[1]There are, however, regions of parameter space in the MSSM within which the effective $hb\bar{b}$ coupling is suppressed due to radiative corrections [8], and consequently BR($h \to \ell\ell$) becomes large.

[2]In the literature, this scenario has also been referred to as the lepton-specific 2HDM [9], leptonic 2HDM [10].

$$V = m_1^2|\phi_q| + m_2^2|\phi_\ell|^2 + (m_{q\ell}^2\phi_q^\dagger\phi_\ell + \text{H.c.}) + \lambda_1(|\phi_q|^2)^2 + \lambda_2(|\phi_\ell|^2)^2 + \lambda_3|\phi_q|^2|\phi_\ell|^2 + \lambda_4|\phi_q^\dagger\phi_\ell|^2 + \frac{\lambda_5}{2}[(\phi_q^\dagger\phi_\ell)^2 + \text{H.c.}]. \quad (2)$$

It is assumed that the parameters of the theory are assigned such that both ϕ_q and ϕ_ℓ acquire nonzero VEVs (which we, respectively, denote v_q and v_ℓ), and that $v_q^2 + v_\ell^2 = v^2 \equiv (174\ \text{GeV})^2$. We define $\tan\beta$ as

$$\tan\beta \equiv v_q/v_\ell, \quad (3)$$

so that large $\tan\beta$ corresponds to small v_ℓ, and therefore to large intrinsic lepton Yukawa couplings. In the broken phase of the theory, the spectrum of the model includes the three massless Goldstone modes which become the longitudinal modes of the $W^\pm$ and Z bosons, as well as five massive scalar degrees of freedom: two CP-even fields h and H, a pseudoscalar A, and a pair of charged fields $H^\pm$. The relationship between the physical CP-even Higgs scalars h, H and the real, neutral degrees of freedom in ϕ_q and ϕ_ℓ is parametrized by the mixing angle α:

$$\begin{pmatrix} H \\ h \end{pmatrix} = \sqrt{2}\begin{pmatrix} \cos\alpha & \sin\alpha \\ -\sin\alpha & \cos\alpha \end{pmatrix}\begin{pmatrix} \text{Re}[\phi_\ell^0 - v_\ell] \\ \text{Re}[\phi_q^0 - v_q] \end{pmatrix}. \quad (4)$$

In what follows, we will focus primarily on the physics of h, the lightest of these two scalars.

Since the potential given in Eq. (2) includes eight model parameters—λ_i $(i = 1, \ldots, 5)$, m_1^2, m_2^2, and m_{ql}^2—which are subject to the constraint $v_q^2 + v_\ell^2 = (174\ \text{GeV})^2$, seven of these eight parameters may be considered free. In what follows, it will be useful to work in a different, more physically meaningful basis for these parameters:

$$(m_h, m_H, m_A, m_{H^\pm}, \tan\beta, \sin\alpha, \lambda_5), \quad (5)$$

where m_h, m_A, m_H, and $m_{H^\pm}$ are the masses of the corresponding physical Higgs scalars.

In order to study the collider phenomenology of the L2HDM, it will be necessary to characterize how the effective couplings between h and the SM fields differ from their SM values. Eq. (1) indicates that the effective couplings between the fermions and h are given in terms of these mixing angles[3] by

$$\mathcal{L}_{h\bar{f}f} = -\frac{m_u}{\sqrt{2}v}\frac{\cos\alpha}{\sin\beta}h\bar{u}_L u_R - \frac{m_d}{\sqrt{2}v}\frac{\cos\alpha}{\sin\beta}h\bar{d}_L d_R + \frac{m_e}{\sqrt{2}v}\frac{\sin\alpha}{\cos\beta}h\bar{e}_L e_R + \text{H.c.}. \quad (6)$$

Following [17], we can define a set of parameters η_i which represent the ratios of these effective couplings to their SM values. At tree level,

$$\eta_u = \eta_d = \frac{\cos\alpha}{\sin\beta}, \qquad \eta_\ell = -\frac{\sin\alpha}{\cos\beta}. \quad (7)$$

Similarly, one can also define η-parameters for the trilinear couplings of h with the electroweak gauge bosons, with the result that

$$\eta_W = \eta_Z \equiv \eta_V = \sin(\beta - \alpha). \quad (8)$$

Since a certain set of effective couplings whose leading contributions occur at one loop—namely hgg and $h\gamma\gamma$—are also relevant to the collider phenomenology of Higgs bosons, it is worth deriving η-factors for them as well. The effective operators that give rise to hgg and $h\gamma\gamma$ are [18]

$$\left(\sum_q \eta_q F_{1/2}(\tau_q)\right)\frac{h}{\sqrt{2}v}\frac{\alpha_3}{8\pi}G^a_{\mu\nu}G^{a\mu\nu}, \quad (9)$$

$$\left(\eta_W F_1(\tau_W) + 3\sum_q Q_q^2\eta_q F_{1/2}(\tau_q) + \sum_\ell \eta_\ell F_{1/2}(\tau_\ell)\right) \times \frac{h}{\sqrt{2}v}\frac{\alpha}{8\pi}F_{\mu\nu}F^{\mu\nu}, \quad (10)$$

where $\tau_i = 4m_i^2/m_h^2$, Q_q is the electric charge of quark q, and

$$F_{1/2}(\tau) = -2\tau[1 + (1-\tau)f(\tau)] \quad (11)$$

$$F_1(\tau) = 2 + 3\tau + 3\tau(2-\tau)f(\tau) \quad (12)$$

and

$$f(\tau) = \begin{cases} \arcsin^2(1/\sqrt{\tau}) & \tau \geq 1 \\ -\frac{1}{4}[\log(\eta_+/\eta_-) - i\pi]^2 & \tau < 1 \end{cases} \quad (13)$$

with $\eta_\pm = (1 \pm \sqrt{1-\tau})$. When $F_1(\tau_i)$ and $F_{1/2}(\tau_i)$ are complex (which occurs when $m_h > 2m_i$), it corresponds to internal lines going on shell. This allows us to define a scaling factor for each of these effective vertices:

$$\eta_g = \frac{\sum_q \eta_q F_{1/2}(\tau_q)}{\sum_q F_{1/2}(\tau_q)} = \eta_q \quad (14)$$

$$\eta_\gamma = \frac{\eta_W F_1(\tau_W) + 3\sum_q Q_q^2\eta_q F_{1/2}(\tau_q) + \sum_\ell \eta_\ell F_{1/2}(\tau_\ell)}{F_1(\tau_W) + 3\sum_q Q_q^2 F_{1/2}(\tau_q) + \sum_\ell F_{1/2}(\tau_\ell)}. \quad (15)$$

Since $F_{1/2}(\tau_f)$ has an overall m_f^2 prefactor (from the τ_f), the contribution from top quarks running in the loops will still dominate over the contribution from leptons unless $\eta_\ell/\eta_q \sim 10^4$; thus the lepton loops generally can be neglected. It is worth noting that since the effective Higgs-gluon-gluon coupling receives contributions solely from

[3]Note that these expressions depend on the conventions (3) and (4) used in defining α and β, and hence frequently differ from source to source within the literature.

quark loops, $\eta_g = \eta_q$ to leading order in α_s, whereas η_γ depends on η_q, η_ℓ, and η_W in a nontrivial way.

The mixing angles α and β are constrained by several theoretical consistency conditions, as well as a number of experimental constraints. We will put off discussion of the latter until Sec. III and focus on the former. First of all, we require that the Higgs sector not be strongly coupled, in the sense that all λ_i may be considered perturbatively small (i.e. $\lambda_i < 4\pi$ for all $i = 1, \ldots, 5$) and that the S-matrix satisfies all relevant tree-unitarity constraints. This implies that the quartic couplings λ_i appearing in Eq. (2) must satisfy [19]

$$\begin{aligned}
\frac{1}{2}(3(\lambda_1 + \lambda_2) \pm \sqrt{9(\lambda_1 - \lambda_2)^2 + 4(2\lambda_3 + \lambda_4|)^2}) &< 8\pi, \\
\lambda_3 + 2\lambda_4 \pm |\lambda_5| &< 8\pi \\
\frac{1}{2}(\lambda_1 + \lambda_2 \pm \sqrt{(\lambda_1 - \lambda_2)^2 + 4|\lambda_5|^2}) &< 8\pi, \\
\lambda_3 \pm \lambda_4 &< 8\pi \\
\frac{1}{2}(\lambda_1 + \lambda_2 \pm \sqrt{(\lambda_1 - \lambda_2)^2 + 4|\lambda_5|^2}) &< 8\pi, \\
\lambda_3 \pm |\lambda_5| &< 8\pi.
\end{aligned} \tag{16}$$

Perturbativity constraints also apply to the Yukawa couplings y_u, y_d, and y_e appearing in Eq. (1), which are modified from their SM values according to Eq. (6). However, we will be focusing primarily on regions of parameter space with $\tan\beta$ in the range $1 < \tan\beta \lesssim 20$, for which these constraints are satisfied. In addition to these perturbativity constraints, we must also require that the scalar potential given in Eq. (2) is finite at large field values and contains no flat directions. These considerations translate into the bounds [16]

$$\begin{aligned}
&\lambda_{1,2} > 0, \qquad \lambda_3 > -2\sqrt{\lambda_1\lambda_2}, \\
&\lambda_3 + \lambda_4 - |\lambda_5| > -2\sqrt{\lambda_1\lambda_2}.
\end{aligned} \tag{17}$$

In this work, we will be primarily interested in examining situations in which the additional physical scalars $H^\pm$, H, and A are heavy enough to "decouple" from the collider phenomenology of the theory in the sense that the only observable signals of beyond-the-standard-model physics at the LHC at low luminosity involve the light CP-even scalar h. For our present purposes, it will be sufficient to define our "decoupling regime" by the condition that $m_{H^\pm}, m_H, m_A > M$, where M is some high scale. Of course this regime includes the strict decoupling limit in which $M \to \infty$ and the mixing angles satisfy the condition $\alpha \approx \beta - \pi/2$. However, it also includes substantial regions of parameter space within which the values of α and β deviate significantly from this relationship.

The extent of parameter space allowed according to our definition of the decoupling regime is illustrated in Fig. 1.

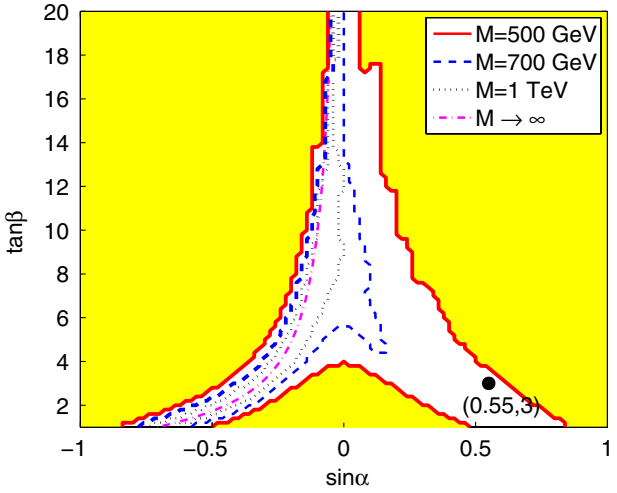

FIG. 1 (color online). The decoupling region of $\sin\alpha$-$\tan\beta$ parameter space within which all perturbativity and vacuum-stability constraints are simultaneously satisfied. The three contours shown correspond to $m_{H^\pm}, m_A, m_H > M$ for $M = 500$ GeV (solid line), $M = 700$ GeV (dashed line), and $M = 1000$ GeV (dotted line). The pure decoupling limit in which $m_{H^\pm}$, m_A, $m_H \to \infty$ is indicated by the dash-dotted line. The dot marks the point ($\sin\alpha = 0.55$, $\tan\beta = 3$), which will be used as a benchmark point in the analysis presented in Sections IV and V. Within the shaded region, at least one of scalars H, A or $H^\pm$ is light (< 500 GeV).

This figure shows the decoupling regions of $\sin\alpha - \tan\beta$ parameter space in which all of the aforementioned constraints are satisfied for a variety of different values of M. Contours corresponding to $M = 500$ GeV, $M = 700$ GeV, and $M = 1$ TeV are displayed, along with a dash-dotted line representing the pure decoupling limit, where $m_{H^\pm}, m_H, m_A \to \infty$ and $\alpha \approx \beta - \pi/2$. The contours in Fig. 1 were obtained by fixing m_h to a particular value (120 GeV) and surveying over the remaining parameters. A given combination of $\sin\alpha$ and $\tan\beta$ is considered to be "allowed" in this sense as long as there exists some combination of model parameters for which $m_{H^\pm}$, m_H, $m_A > M$, and for which all of the constraints in Eqs. (16) and (17) are simultaneously satisfied. It is readily apparent from the figure that sizable regions of parameter space exist within which all constraints are satisfied, yet the masses of all scalars other than h are large enough to effectively decouple from the low-energy effective description of the model. It is also apparent that for $M \gg 1$ TeV, the decoupling region, as we have defined it, approaches the pure decoupling limit.

It is interesting to inquire to what extent the effective Higgs couplings can be modified in the decoupling regime without running afoul of the aforementioned constraints. In the three panels shown in Fig. 2 we plot a number of contours in $\sin\alpha - \tan\beta$ parameter space corresponding to different values of η_ℓ (left), η_q (center) and η_V (right). On each panel, we have also superimposed the $M = 500$ GeV contour from Fig. 1. It is evident from these plots

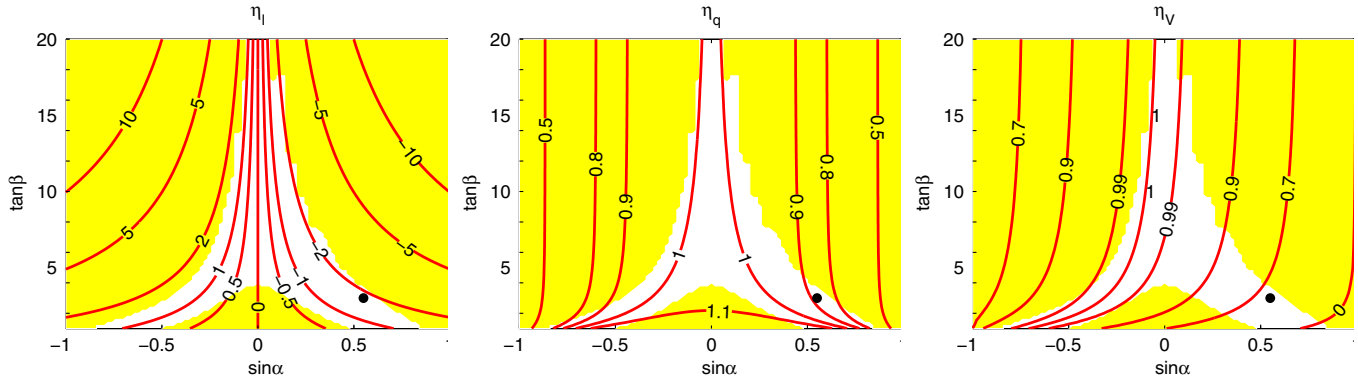

FIG. 2 (color online). Contours for η_ℓ (left), η_q (center), and η_V (right) in $\sin\alpha - \tan\beta$space in the L2HDM. Superimposed on each of these panels is an outline of the region within which all perturbativity and vacuum-stability constraints are simultaneously satisfied for $m_{H^\pm}$, m_H, $m_A > 500$ GeV, as in Fig. 1. The dot marks the benchmark point ($\sin\alpha = 0.55$, $\tan\beta = 3$).

that while η_ℓ, η_q, $\eta_V \to 1$ in the $M \to \infty$ limit, large regions of parameter space are still allowed in the decoupling regime within these η-factors can deviate substantially from unity. The message, then, is that the effective couplings of a light Higgs boson in the decoupling regime do not have to approximate those which correspond to the pure decoupling limit, in which they approach those of a SM Higgs. On the contrary, a wide variety of possibilities for the mixing angles α and β are still open in this regime, and as we shall soon see, many of these possibilities have a dramatic effect on in the collider phenomenology of the scalar h.

III. EXPERIMENTAL CONSTRAINTS

In addition to the perturbativity and vacuum-stability bounds discussed in the previous section, the L2HDM is constrained by additional considerations related to flavor-physics experiment, direct searches, etc. We now proceed to investigate these constraints in an effort to show that they can easily be satisfied in the decoupling regime—even in the region of parameter space most interesting for collider phenomenology, where $\tan\beta$ is large and $\sin\alpha$ deviates substantially from zero.

Let us begin with those bounds related to direct searches for beyond-the-standard-model scalars at LEP. The current direct detection bounds (at 95% CL) for the masses of charged and neutral CP-odd Higgs bosons, as reported by the particle data group [20], are $m_{H^\pm} \geq 78.6$ GeV and $m_A \geq 93.4$ GeV. These clearly present no problem for the model in the decoupling limit considered here.

Far more stringent constraints on models with more than one Higgs doublet can be derived, however, from experimental limits on flavor-violating processes that receive contributions at the one-loop level from diagrams involving charged Higgs bosons. Let us first consider flavor violation in the lepton sector, which is constrained by analyses of $\tau \to \mu\gamma$, $\mu \to e\gamma$, $\tau \to \mu ee$, and $\mu \to e$ conversion in nuclei. In the absence of neutrino masses, the matrix of effective $H^+ \bar{\nu}_i e_j$ couplings is proportional to the charged-lepton mass matrix; hence there is no additional source of lepton-flavor violation (LFV). In the presence of neutrino masses this is no longer true, and nonzero contributions to LFV processes arise at one loop due to diagrams with charged Higgs bosons running in the loop. However, it has been shown [21] that the resultant flavor-violating amplitudes are several orders of magnitude below current experimental bounds. Therefore, even in cases in which the effective $H^+ \bar{\nu} e^-$ coupling receives a substantial $\tan\beta$-enhancement factor, such sources of LFV will not present any phenomenological difficulties.

Now let us turn to consider the situation in the quark sector, where, by contrast, flavor-violation rates can be sizeable. This is because the effective $H^+ \bar{u}_i d_j$ couplings in two-Higgs-doublet models include flavor-violating terms proportional to the off-diagonal elements of the Cabibbo-Kobayashi-Maskawa (CKM) matrix V_{ij}:

$$\mathcal{L}_{H^\pm \bar{f} f'} = -\frac{\cot\beta}{v} V_{ij} \bar{u}_i [m_{u_i} P_L - m_{d_j} P_R] d_j H^+ - \frac{\tan\beta}{v} m_{e_i} \bar{\nu}_i P_R e_i H^+ + \text{H.c.}, \tag{18}$$

As a result, such models are constrained by experimental bounds on $\mathrm{BR}(b \to s\gamma)$, ΔM_K, ΔM_D, ΔM_B, rare kaon decays, etc., which translate into bounds on the model parameters relevant to the charged-scalar sector: $m_{H^\pm}$ and $\tan\beta$. Since the flavor mixing in the charged Higgs couplings to the quark sector is proportional to $\cot\beta$, it is the region where both $\tan\beta$ and $m_{H^\pm}$ are small which is most tightly constrained by these bounds. The most stringent constraints are those associated with $b \to s\gamma$ and with mixing in the $B^0 - \bar{B}^0$ and $K_L - K_S$ systems. In the L2HDM, the same Higgs doublet couples to both up- and down-type quarks, just as it does in type I 2HDM [18,22]; hence the bounds on $m_{H^\pm}$ and $\tan\beta$ due to flavor mixing in the quark sector will be essentially identical to those applicable in type I models. We now turn to review the

bounds from each of these processes, updating the results obtained in [13,14].

The first bounds we consider are those associated with the observed branching ratio for the flavor-violating decay $b \to s\gamma$. The combined result from the CLEO and Belle experiments [20] is

$$\mathrm{BR}(b \to s\gamma) = (3.3 \pm 0.4) \times 10^{-4}. \tag{19}$$

This is consistent with the expected standard model result $\mathrm{BR}^{\mathrm{SM}}(b \to s\gamma) = 3.32 \times 10^{-4}$. In models with a nonminimal Higgs sector, additional contributions to the amplitude for $b \to s\gamma$ arise at the loop level from diagrams involving virtual charged Higgs bosons, as discussed above. These diagrams are compiled in Fig. 3 (SM contributions to this amplitude come from diagrams of the same sort, but with $W^{\pm}$ in place of $H^{\pm}$.) The rate for the process can be calculated in the usual manner. After incorporating the effect of QCD corrections (which can be quite large [23]), one finds that [13,24]

$$\Gamma(b \to s\gamma) = \frac{\alpha G_F^2 m_b^5}{128\pi^4} |c_7(m_b)|^2, \tag{20}$$

where $c_7(m_b)$ is the coefficient of the effective operator

$$\mathcal{O}_7 \equiv F_{\mu\nu} \bar{s}_L \sigma^{\mu\nu} b_R \tag{21}$$

in the conventions of Ref. [25], evaluated at the scale m_b. This coefficient takes the form

$$c_7(m_b) = \left(\frac{\alpha_3(M_W)}{\alpha_3(m_b)}\right)^{16/23} \times \left[c_7(M_W) - \frac{3c}{10}\left[\left(\frac{\alpha_3(M_W)}{\alpha_3(m_b)}\right)^{10/23} - 1\right] - \frac{3x}{28}\left[\left(\frac{\alpha_3(M_W)}{\alpha_3(m_b)}\right)^{28/23} - 1\right]\right], \tag{22}$$

where the weak-scale amplitude function $c_7(M_W)$ in the L2HDM is given by

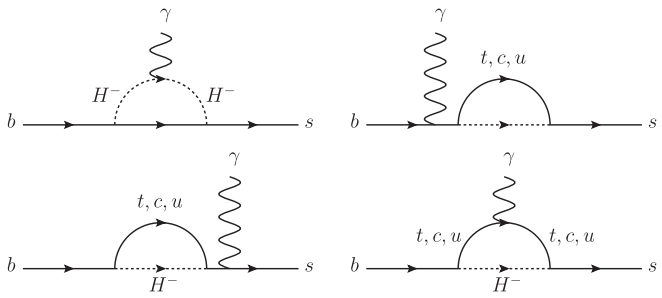

FIG. 3. The leading-order diagrams that yield a contribution to the $b \to s\gamma$ amplitude due to the presence of massive, charged-Higgs bosons in loops. The standard-model contribution to this process involves similar diagrams with H^- replaced by W^-.

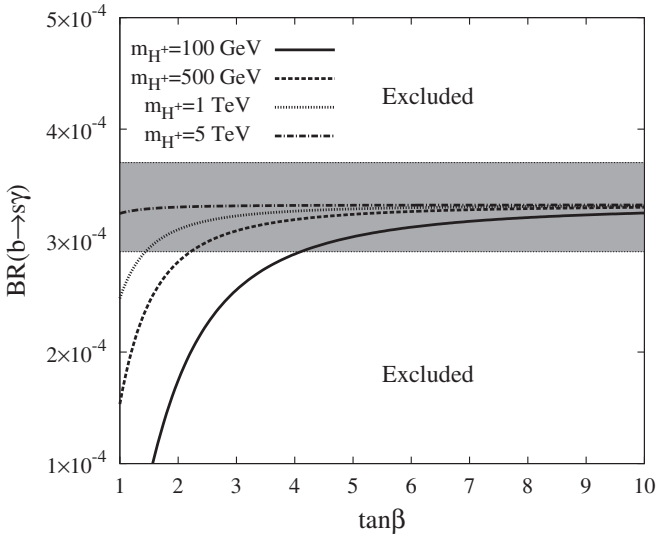

FIG. 4. Constraints on the charged-Higgs mass and $\tan\beta$ from $\mathrm{BR}(b \to s\gamma)$ measurements. The shaded horizontal band corresponds to the experimentally-allowed 1σ region from CLEO and Belle [20]. The curves plotted here correspond to $m_{H^\pm} = 100$ GeV (solid line), $m_{H^\pm} = 500$ GeV (dashed line), $m_{H^\pm} = 1$ TeV (dotted line), and $m_{H^\pm} = 5$ TeV (dash-dotted line).

$$c_7(M_W) = \sum_{i=u,c,t} V_{is}^* V_{ib} [G_W(x_i) - \cot^2\beta G_H^{(1)}(y_i) + \cot^2\beta G_H^{(2)}(y_i)]. \tag{23}$$

In these formulas, $\alpha_3 = g_3^2/4\pi$ and $\alpha = e^2/4\pi$, $x_i = m_{q_i}^2/M_W^2$, $y_i = m_{q_i}^2/m_{H^\pm}^2$, G_F is the Fermi constant, V_{ij} are elements in the CKM matrix, and $c = 232/81$. The functions $G_W(x)$, $G_H^{(1)}(x)$, and $G_H^{(2)}(x)$, which represent the loop integral contributions to the $b \to s\gamma$ amplitude, are given in [13].

The constraints on $m_{H^\pm}$ and $\tan\beta$ from $b \to s\gamma$ are displayed in Fig. 4. Each curve therein represents the value of $\mathrm{BR}(b \to s\gamma)$ for a given choice of $m_{H^\pm}$ as a function of $\tan\beta$. Note that for the case under consideration here, in which $m_{H^\pm} > 500$ GeV, the experimental constraints are satisfied as long as $\tan\beta \gtrsim 2$.

Constraints on $m_{H^\pm}$ and $\tan\beta$ can also be obtained from limits on the observed mixing in the mesonic $B^0 - \bar{B}^0$ and $K_L - K_S$ systems. The diagrammatic contributions to $B^0 - \bar{B}^0$ mixing are shown in Fig. 5, and these contributions translate into shift in the mass-splitting ΔM_B between B^0 and $\bar{B}^0$. In the L2HDM, this splitting, including SM contributions, is given by [13]

$$\Delta M_B = \frac{G_F^2 M_W^2}{6\pi^2} m_B f_B^2 B_B \sum_{i=u,c,t} |(V_{ib} V_{id}^*)^2| \eta_{\mathrm{QCD}} [A_{WW}(x_t) + \cot^4\beta A_{HH}(x_t, x_H, x_b) + \cot^2\beta A_{WH}(x_t, x_H, x_b)], \tag{24}$$

where the x_i are defined as below Eq. (23), f_B is the

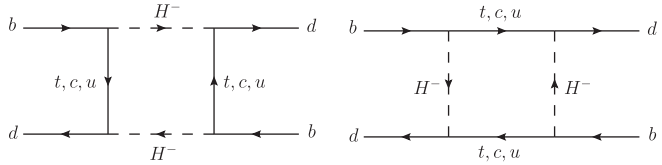

FIG. 5. Box diagrams that contribute to ΔM_B in the $B^0 - \bar{B}^0$ system via charged-Higgs exchange. Diagrams in which one or both of the H^- propagators is replaced by a W^- propagator also contribute. The box diagrams for transitions in the $K_L - K_S$ system, etc. are analogous.

B-meson decay constant, B_B is the "bag factor" (which encompasses all deviations from the vacuum saturation approximation). Expressions for the factor $\eta_{\rm QCD}$, which accounts for QCD effects, along with the functions $A_{WW}(x_t)$, $A_{HH}(x_t, x_H, x_b)$, and $A_{WH}(x_t, x_H, x_b)$ can be found in [13].

As for f_B and B_B, there is a good deal of uncertainty as to their precise numerical values. Since they appear in Eq. (24) in the combination $f_B B_B^{1/2}$, it is easier simply to deal with the uncertainty in this single quantity. Estimates of $f_B B_B^{1/2}$ have been made using a variety of lattice QCD sum rules in conjunction with experimental evidence on heavy meson decays from SLAC, and the uncertainties in their values depend on the summation methods employed and the assumptions made. Following [13,26], we take the range of uncertainty to be

$$100 \text{ MeV} \lesssim f_B B_B^{1/2} \lesssim 180 \text{ MeV}. \tag{25}$$

Instead of dealing with ΔM_B directly, it is easier to deal with the combination $x_d \equiv \Delta M_B/\Gamma_B$, since the time-integrated mixing probability in the $B^0 - \bar{B}^0$ system depends on this combination of variables. The accepted experimental value for x_d, as reported by the Heavy Flavor Averaging Group, is $x_d = 0.776 \pm 0.008$ [20]. Using the observed lifetime of the B^0 meson ($\tau_B = 1.530 \times 10^{-12}$ sec) and the expression in Eq. (24), one may obtains a theoretical value for x_d, which can be compared to this experimental result.

In Fig. 6, we show how the $B^0 - \bar{B}^0$ mixing bound constrains $m_{H^\pm}$ and $\tan\beta$. As there is a large uncertainty in $f_B B_B^{1/2}$ [Eq. (25)], and in fact one far larger than that associated with the measured value of x_d, the theoretical prediction for a given choice of $m_{H^\pm}$ translates into a broad band in $\tan\beta - x_d$ space, rather than a thin line. In Fig. 6, the upper and lower bounds of each such band are demarcated by a pair of thick, dark lines of the same type (solid, dotted and dot-dashed). The thin, shaded, horizontal stripe represents the experimentally-allowed window. If any part of this stripe falls within the band corresponding to a given value of $m_{H^\pm}$ for a given $\tan\beta$, that parameter combination is permitted by the ΔM_B constraint. We see from the plot that this constraint only becomes relevant for very small values of $\tan\beta \sim 1$, and thus is not particularly stringent.

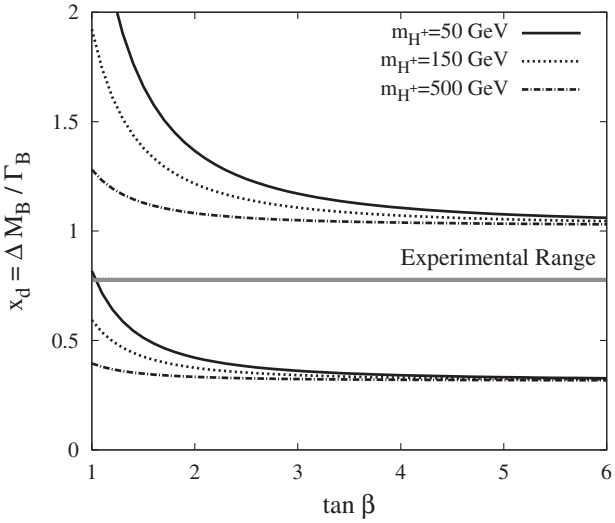

FIG. 6. Bounds on $m_{H^\pm}$ and $\tan\beta$ from mixing in the $B^0 - \bar{B}^0$ system, plotted as a function of $\tan\beta$. The thin shaded region represents the experimentally-allowed 1σ range for $x_d = \Delta M_B/\Gamma_B$ [20]. Each pair of thick curves represents the upper and lower limits on the theoretical value of x_d (due to uncertainties in hadronic matrix elements, etc.) for three different choices of $m_{H^\pm}$: 50 GeV (solid lines), 150 GeV (dotted lines), and 500 GeV (dot-dashed lines). A certain combination of $\tan\beta$ and $m_{H^\pm}$ is permitted as long as any part of the experimentally-allowed range falls between the lines corresponding to the upper and lower theoretical limits.

Similar calculations to those outlined above for the $B^0 - \bar{B}^0$ system can also be performed for mixing in the $K_L - K_S$ and $D^0 - \bar{D}^0$ systems [13]. In addition, limits can also be derived on the CP-violating parameters ϵ and ϵ'. However, due to large theoretical uncertainties in the hadronic matrix elements, the resulting bounds on new physics from these considerations are not particularly stringent in the L2HDM, especially when $\tan\beta > 1$ [14].

Experimental bounds on leptonic charged-meson decays—$D_S^\pm \to \mu^\pm\nu$, $D_S^\pm \to \tau^\pm\nu$, $K^\pm \to \mu^\pm\nu$, $B^\pm \to \tau^\pm\nu$ etc.—can also be used to constrain 2HDM [27]. In general, the partial width for the leptonic decay of a given meson is modified by a $\tan\beta$-dependent factor $r_{M\ell}$, which in many scenarios (e.g. type II models) can be quite sizeable when $\tan\beta$ is large [28]. In the L2HDM, however, the $r_{M\ell}$ are independent of $\tan\beta$ due to the cancellation of the $\tan\beta$ factors between the quark and the lepton couplings. As a result the model is essentially unconstrained by these considerations. Experimental limits on the rates for leptonic decays such as $\tau \to \mu\bar{\nu}\nu$ can also constrain models with enhanced Higgs couplings to leptons [29]. However, such constraints only become relevant when the charged-Higgs mass is $\mathcal{O}(100$ GeV) or lower, or when $\tan\beta$ is extremely large, and thus have little bearing on the decoupling regime studied here.

The above analysis shows that in the decoupling region (as we have defined it), where $m_{H^\pm} > 500$ GeV, all con-

straints from direct charged-Higgs searches, neutral meson mixing, CP-violation, charged-meson decay, etc. can be satisfied as long as $\tan\beta$ is greater than ~ 2. This is mainly due to the fact that in the L2HDM, there is no new source of flavor violation except the SM CKM matrix. The effective couplings between $H^{\pm}$ and the SM quarks are proportional to $\cot\beta$, which implies that the most stringent constraints become weaker as $\tan\beta$ increases. Thus, we conclude that experimental constraints from flavor violation, direct searches, etc. do not pose any significant issues for the L2HDM as long as the charged Higgs scalars are heavy. (Indeed, a relatively low value of $\tan\beta \approx 3$ and a charged Higgs light enough to be discovered at the LHC are by no means incompatible.) This is true even in the region of parameter space most interesting for collider physics, in which both $\sin\alpha$ and $\tan\beta$ are large, and the effective couplings between the lightest CP-even Higgs and the SM leptons differ drastically from their SM values.

IV. BRANCHING RATIOS AND CROSS SECTIONS

We now turn to examine the effect of these coupling modifications on the production cross sections and decay widths of a light Higgs boson. Since the overall amplitudes for Higgs decays into any two-particle final state X scale as $|\eta_X|^2$ (i.e., the appropriate η-factor for that final state), the associated branching ratios scale like

$$\frac{\mathrm{BR}(h \to X)}{\mathrm{BR}^{\mathrm{SM}}(h \to X)} = |\eta_X|^2 \frac{\Gamma_{\mathrm{tot}}^{\mathrm{SM}}(h)}{\Gamma_{\mathrm{tot}}(h)} = |\eta_X|^2 \left(\sum_i |\eta_{Y_i}|^2 \mathrm{BR}^{\mathrm{SM}}(h \to Y_i) \right)^{-1}. \tag{26}$$

In order to provide a concrete example of the effect such a modification can have on Higgs phenomenology, let us focus on a particular benchmark point: $\sin\alpha = 0.55$, $\tan\beta = 3$, which we have indicated by a dot in Fig. 1. We pick this particular point as a benchmark because it yields only a moderate deviation from the SM couplings and is consistent with the bounds (16) and (17) when $m_{H^{\pm}}$, m_H, $m_A > 500$ GeV. The η-factors corresponding to this particular point are

$$\eta_q = \eta_g = 0.88, \qquad \eta_\ell = -1.74, \qquad \eta_V = 0.62, \qquad \eta_\gamma = 0.54. \tag{27}$$

Figure 7 illustrates the effect of this coupling-constant modification on the branching ratios of a light, CP-even Higgs scalar. In the left-hand panel, we have plotted the SM branching ratios for a number of Higgs decay processes as a function of m_h. All branching ratios used in the construction of the figure were calculated using HDECAY [30]. In the right-hand panel, we have plotted branching ratios for the same set of processes in the L2HDM at our chosen benchmark point. It is evident that even this moderate modification of the couplings has a dramatic effect on the decay behavior of a light Higgs: for example, the rates for $\mathrm{BR}(h \to \tau^+\tau^-)$ and $\mathrm{BR}(h \to b\bar{b})$ are on the same order. Since $h \to b\bar{b}$ is the dominant decay channel for a Higgs boson with a mass in the range 114 GeV $\lesssim m_h \lesssim$ 140 GeV, this clearly represents a substantial effect on Higgs phenomenology. It is also worth noting that $\mathrm{BR}(h \to \mu^+\mu^-)$ and $\mathrm{BR}(h \to \gamma\gamma)$ are also on the same order for this choice of parameters. This suggests that processes involving direct decays of a light Higgs boson to a pair of high-p_T muons could play an important role in the collider phenomenology of the light Higgs—a suggestion we will explore further in Sec. V. The branching ratios for a number of other decay channels relevant to the study of a

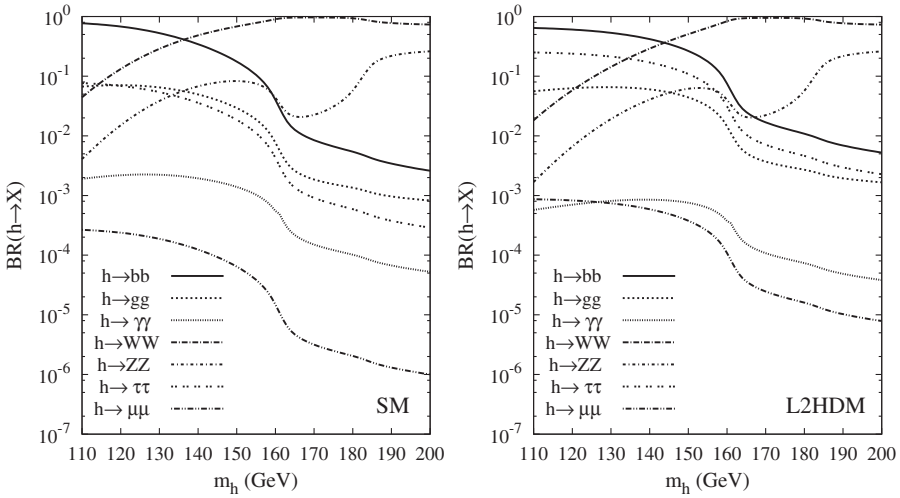

FIG. 7. Plots of the Branching ratios for the a number of two-body decays of the Higgs boson, both in the SM (left panel) and in the L2HDM (right panel) for the benchmark point ($\sin\alpha = 0.55$, $\tan\beta = 3$). Note that $\mathrm{BR}(h \to \tau^+\tau^-)$ and $\mathrm{BR}(h \to b\bar{b})$ are on the same order, as are $\mathrm{BR}(h \to \mu^+\mu^-)$ and $\mathrm{BR}(h \to \gamma\gamma)$.

light SM Higgs boson at the LHC, such as $h \to \gamma\gamma$, are clearly suppressed here relative to their SM values.

The effect of the coupling modifications on the total Higgs width is shown in Fig. 8. Here, we have plotted the ratio of the total Higgs width $\Gamma_{\rm tot}(h)$ to its SM value for three different points in the allowed region of $\sin\alpha - \tan\beta$ parameter space as a function of m_h. The first of these points is our chosen benchmark ($\sin\alpha = 0.55$, $\tan\beta = 3$), for which $\Gamma_{\rm tot}(h)$ (indicated by the solid line) is slightly lower than its SM value due to the suppression of $\Gamma(h \to b\bar{b})$ when m_h is small. When m_h increases and decays to electroweak gauge bosons begin to dominate the Higgs width, $\Gamma_{\rm tot}(h)$ drops even further, since $\eta_V < \eta_q$ at this point [see Eq. (27)]. The second of these points, ($\sin\alpha = -0.1$, $\tan\beta = 10$), is located very near the "pure decoupling" line in Fig. 1; hence for this point $\Gamma_{\rm tot}(h)$ (indicated by the dotted line) is essentially equal to $\Gamma^{\rm SM}_{\rm tot}(h)$. At the third point, ($\sin\alpha = 0.3$, $\tan\beta = 7$), a substantial enhancement in $\Gamma(h \to \tau\tau)$ overcomes the suppression factor in $\Gamma(h \to b\bar{b})$, and consequently $\Gamma_{\rm tot}(h) > \Gamma^{\rm SM}_{\rm tot}(h)$ for $m_h \lesssim 140$ GeV (as indicated by the dash-dotted line). For larger values of m_h, gauge-boson decays once again dominate the Higgs width, which becomes suppressed relative to its SM value. Even in the most extreme cases permitted by the model consistency constraints outlined in Sec. II, however, $\Gamma_{\rm tot}(h)/\Gamma^{\rm SM}_{\rm tot}(h) \lesssim 2$. This implies that the narrow-width approximation remains valid over the Higgs mass range $114\ {\rm GeV} \lesssim m_h \lesssim 140\ {\rm GeV}$, which will be the mass region of primary focus of the present work.

Since we have shown that the narrow-width approximation to be valid, we can proceed in a straightforward manner from the decay width calculations above to determine how the cross sections for full collider processes are modified. In this approximation, one assumes that essentially all the Higgs bosons produced in any such process are produced on shell. This allows one to approximate the cross section for any process of the form $Y \to h \to X$ by

$$\sigma(Y \to h \to X) \approx \sigma(Y \to h) \times {\rm BR}(h \to X). \tag{28}$$

Furthermore, if the SM production cross section $\sigma^{\rm SM}(Y \to h)$ for the process is known, one can use the fact that $\sigma(Y \to h) \propto \Gamma(h \to Y)$ to obtain the relation

$$\begin{aligned}\frac{\sigma(Y \to h \to X)}{\sigma^{\rm SM}(Y \to h \to X)} &= \frac{\Gamma(h \to Y)}{\Gamma^{\rm SM}(h \to Y)} \times \frac{{\rm BR}(h \to X)}{{\rm BR}^{\rm SM}(h \to X)} \\ &= \frac{{\rm BR}(h \to Y)}{{\rm BR}^{\rm SM}(h \to Y)} \times \frac{{\rm BR}(h \to X)}{{\rm BR}^{\rm SM}(h \to X)} \\ &\quad \times \frac{\Gamma_{\rm tot}(h)}{\Gamma^{\rm SM}_{\rm tot}(h)},\end{aligned} \tag{29}$$

which allows us to calculate the cross sections for these overall processes in the modified model.

For the benchmark point that we have chosen ($\sin\alpha = 0.55$, $\tan\beta = 3$), the cross sections for most of the conventional Higgs search modes at the LHC are suppressed relative to their SM values, due to the suppressed Higgs couplings to quarks and to gauge bosons. Many of the processes in which the Higgs decays directly to charged-lepton pairs, on the other hand, are substantially enhanced. We will discuss the implications these modifications can have for Higgs searches in detail in Sec. VI.

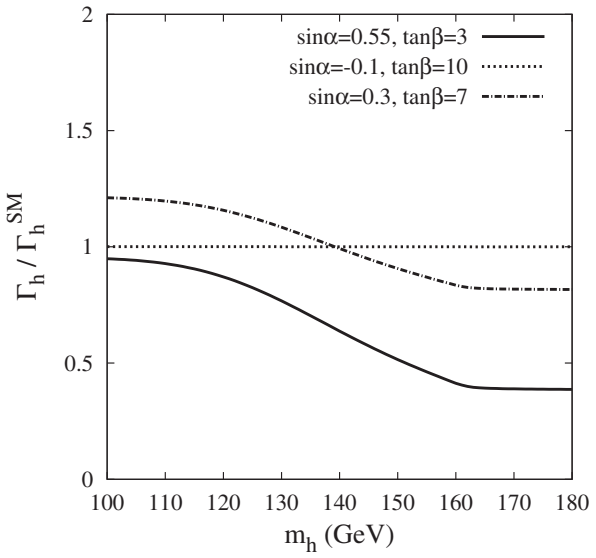

FIG. 8. Plot of the ratio of the total width of the Higgs boson in the leptophilic 2HDM to that of a SM Higgs for a representative sample of points in $\sin\alpha - \tan\beta$parameter space as a function of the Higgs mass m_h.

V. LHC SIGNATURES OF A LEPTOPHILIC HIGGS BOSON

One of the most interesting aspects of the L2HDM is that in certain regions of parameter space, new channels for the discovery of a light Higgs boson can open up. In particular, when the effective coupling between h and the SM leptons is substantially increased while its couplings to SM quarks and/or electroweak gauge bosons are not dramatically suppressed, a number of processes in which the Higgs boson decays directly to a pair of high-p_T leptons can become far more important for the discovery of a light Higgs than they are in the SM. In our analyses, we focus on the discovery of h in the light-to-intermediate-mass region $120\ {\rm GeV} < m_h < 140\ {\rm GeV}$. For heavier Higgs bosons, $h \to WW^*$, ZZ^* dominates and leptonic Higgs decays play a less important role. In the decoupling limit case studied here, in which the additional Higgs scalars $H^\pm$, H, and A are heavy, such processes might well constitute the only evidence for physics beyond the standard model accessible within the first 30 fb^{-1} of integrated luminosity at the LHC, and are therefore of crucial importance. This situation is quite different from the one studied in Ref. [10], in which some of these additional scalars are light and play a significant role in collider phenomenology.

Since the largest leptonic contribution to the Higgs total width comes from $h \to \tau\tau$, processes involving Higgs decays directly to tau leptons will play a significant role in the collider phenomenology of the L2HDM. However, the analysis of such processes is complicated by subtleties associated with tau decay. Each τ lepton can decay either leptonically or hadronically, with respective branching ratios [20], $\mathrm{BR}_\tau^{\mathrm{lep}} \simeq 35.20\%$ and $\mathrm{BR}_\tau^{\mathrm{had}} \simeq 64.80\%$. We will henceforth denote a hadronically-decaying tau as τ_h and a leptonically-decaying one as τ_ℓ. For processes involving CP-even Higgs boson decays into a $\tau\tau$ pair, there are two final states which permit successful identification of both taus: $e\mu + \not{E}_T$ and $\tau_h\ell + \not{E}_T$, where $\ell = e, \mu$. Final states resulting from fully hadronic decays have a large background from dijet processes with narrow jets misidentified as taus. Final states involving two leptons of like flavor ($e^+e^- + \not{E}_T$ and $\mu^+\mu^- + \not{E}_T$) are also less useful due to the overwhelming SM background from $Z/\gamma^* \to \ell^+\ell^-$ processes.

A hadronically-decaying tau will decay into either a ''one-prong'' (approximately 77% of the time) or ''three-prong'' (approximately 23% of the time) final state. These final states involve narrow, well-collimated jets including one or three charged pions, respectively. The identification of a jet as coming from a hadronically-decaying τ, as opposed to some QCD process, is far from trivial. One of the principal discrimination variables is jet radius R_{EM} (see [31] for more details regarding τ identification). At the Tevatron (Run II), $\epsilon_{\tau_h} \approx 35\%$–$40\%$ for a $p_T^\tau > 20$ GeV cut. At the LHC, a τ identification efficiency of around 50%–60% is expected [31].

Processes involving direct decays of h to muon pairs can also be of interest for Higgs discovery in the L2HDM. The disadvantage of such channels for Higgs searches, relative to those involving direct decays to taus, is the suppressed branching ratio. Since Yukawa-coupling universality dictates that $y_\mu/y_\tau \propto m_\mu/m_\tau$, both in the SM and in the L2HDM, $\mathrm{BR}(h \to \mu\mu) \ll \mathrm{BR}(h \to \tau\tau)$. However, this is compensated for to a great extent by the fact that the dimuon signal is exceptionally clean. Indeed, the muon identification efficiency at the LHC is more that 90% [5,6]. In addition, the measurement of muon momenta allows for a precise reconstruction of the Higgs mass within ± 2.5 GeV. This permits the implementation of an extremely efficient cut on $M_{\mu\mu}$, the invariant mass of the muon pair, and a substantial reduction in background levels for all channels involving direct Higgs-boson decays to muon pairs.

We now turn to address the prospects for detecting a light SM-like CP-even Higgs boson at the LHC on a channel-by-channel basis. In the present work, as discussed in Sec. II, we will assume generation universality among the lepton Yukawa couplings. Therefore, we will ignore the $h \to ee$ channel and focus only on $h \to \tau\tau$ and $h \to \mu\mu$. The channels of primary interest, then, are those in which the Higgs is produced by gluon fusion, weak-boson fusion, or $t\bar{t}h$ associated production and decays to either $\mu^+\mu^-$ or $\tau^+\tau^-$. Associated $W^\pm$ and Z production processes generally have smaller rates, but may also potentially be of interest, and as such we briefly discuss them as well. Bottom-quark-fusion processes with a leptonically-decaying Higgs boson [32], while potentially interesting for type II 2HDM in which the $h\bar{b}b$ vertex receives a large $\tan\beta$-enhancement, are less useful in the L2HDM, since the effective down-type quark couplings are suppressed in that scenario rather than enhanced. In this section, we briefly summarize the results of the existing studies of the leptonic-Higgs-decay channels at the LHC, with an eye toward their utility for the discovery of a leptophilic Higgs.

A. $qq' \to qq'h(h \to \tau\tau)$

We begin with a discussion of the weak-boson-fusion process $qq' \to qq'h(h \to \tau\tau)$, which is the only channel involving direct Higgs-boson decay to a pair of charged leptons that contributes significantly to the Higgs discovery potential in the SM. Indeed, it is a particularly promising channel for SM Higgs discovery in the intermediate-mass region ($125\ \mathrm{GeV} \lesssim m_h \lesssim 140\ \mathrm{GeV}$) [4], and an even more promising one in scenarios with enhanced Higgs couplings to leptons [33]. Discriminating between signal and SM background can be facilitated by requiring that events have two leading tagging jets in the forward-backward direction and imposing a minijet veto in the central region of the detector. A great deal of attention has been devoted to this channel, with an emphasis on $\tau_h\tau_\ell$ and $\tau_\ell\tau_\ell$ final states. Combining all channels, a statistical significance of more than 5σ can be reached for Higgs masses around 120–130 GeV with 30 fb^{-1} of integrated luminosity at ATLAS [1]. The detection prospects are similar at CMS [2].

B. $gg \to h \to \tau\tau$

The prospects for detecting a light, SM Higgs boson produced by gluon fusion and decaying to $\tau^+\tau^-$ at the Tevatron were examined in Ref. [34]. In order to effectively reconstruct the Higgs mass from the various final-state particles produced during tau decay, it is necessary to focus on events in which the transverse momentum of the tau pair is nonzero; hence the authors elected to focus on the process $p\bar{p} \to hj \to \tau^+\tau^- j$. Taking into account both the S/B and $S/\sqrt{B}$ ratios, $\tau_h\tau_\ell$ turns out to be the most promising channel for signal identification, but that an integrated luminosity of 14 fb^{-1} would be needed at the Tevatron in order to exclude a 120 GeV SM Higgs boson at the 95% C.L. However, preliminary studies at ATLAS [35] indicate that this will be a promising channel in which to look for a Higgs boson with enhanced coupling to leptons at the LHC.

C. $tth(h \to \tau\tau)$

This process was examined in a standard model context in [36]. In order to be able to reconstruct the two top quarks effectively, the authors restricted their analysis to cases in which one of the W bosons produced during top decay decays leptonically, while the other decays hadronically. Only events with hadronic tau decays were considered, as reconstructing both tops proves to be slightly easier in this scenario. Thus the overall process of interest is $pp \to t\bar{t}h \to bbjj\ell\tau_h\tau_h + \not{E}_T$. Since the production cross section drops quickly with increased Higgs mass, this channel is only important when the Higgs is light. For m_h around 120 GeV, a statistical significance of 4σ can be obtained with 100 fb^{-1} of integrated luminosity. In [37], semileptonic tau decays were considered—in particular, decays of the form $pp \to t\bar{t}h \to bbjj\ell\tau_h\tau_\ell + \not{E}_T$, and it was found that such a process could provide evidence for a 120 GeV Higgs boson at the 2.7σ level for an integrated luminosity of 30 fb^{-1}.

D. $qq' \to qq'h(h \to \mu\mu)$

The weak boson fusion process $qq' \to qq'h(h \to \mu\mu)$ was analyzed in [38]. After the appropriate cuts on the tagging jets are imposed, the leading SM background comes from irreducible Zjj or $\gamma^* jj$ processes, with the Z/γ^* decaying to muon pairs. Because of the extremely suppressed SM $h \to \mu\mu$ branching ratio, an integrated luminosity of $\mathcal{O}(300$ fb$^{-1})$ or more is generally required to claim a 3σ discovery for a Higgs mass less than 140 GeV. In the L2HDM, however the detection prospects can be substantially improved if $\eta_V \sim 1$ and $\eta_\ell \gg 1$.

E. $gg \to h \to \mu\mu$

The prospects for the detection of a light Higgs boson of 110 GeV $\leq m_h \leq$ 140 GeV produced by gluon fusion and decaying directly into $\mu^+\mu^-$ were discussed in [39]. The irreducible background for $gg \to h \to \mu\mu$ is dominated by the Drell-Yan processes $q\bar{q} \to Z^*/\gamma^* \to \mu\mu$. The sharp invariant-mass resolution of the muon pair allows for a substantial reduction in this background via a stringent cut on $M_{\mu\mu}$. Consequently, a significance level similar to that in the WBF channel as discussed in [38] can be attained in this channel as well.

F. $tth(h \to \mu\mu)$

The prospects for discovering a standard model Higgs boson in the $tth(h \to \mu\mu)$ channel were recently studied in [40]. This channel tends to be more important when the Higgs mass is light (around 120 GeV) since the production cross section drops quickly for a heavier Higgs. The primary irreducible backgrounds, which come from $t\bar{t}Z$ and $t\bar{t}\gamma^*$ production, with the Z/γ^* decaying into a muon pair, can be reduced quite effectively by a cut on that muon pair's invariant mass. Additional, reducible backgrounds such as $Zb\bar{b}jjjj$ can be effectively eliminated by reconstructing the masses of both top quarks, which is possible in the case where the tops decay either fully hadronically or semileptonically.

The statistical significances for the $tth(h \to \mu\mu)$ channel are of roughly the same order as those in the $gg \to h \to \mu\mu$ and $qq' \to qq'h(h \to \mu\mu)$ channels, and hence could contribute significantly to the discovery potential for a light Higgs scalar with enhanced couplings to leptons.

G. $Wh/Zh(h \to \tau^+\tau^-)$ and $Wh/Zh(h \to \mu^+\mu^-)$

Higgs production via the processes $pp \to Wh$ and $pp \to Zh$ could also potentially play a role in the discovery of a leptophilic Higgs, though the prospects in these channels are not as favorable as the other, aforementioned ones. SM cross sections for these processes, taking into account the leptonic decay of the Higgs boson, are given in Table I for the case in which $m_h = 120$ GeV. These were determined from leading-order results obtained using MADGRAPH [41] and modified by the appropriate K-factors: $K_S = 1.27$ for signal [42], $K_{BG} = 1.7$ for background [43]. For processes in which the Higgs decays to $\mu^+\mu^-$, the signal is clearly too small to be of any use. However, for processes involving decays to $\tau^+\tau^-$, the signal is only about a factor of $\sim$25 smaller than the background. By optimizing cuts to eliminate the SM background, this channel might potentially be of use—particularly if BR$(h \to \tau\tau)$ is enhanced, as in the L2HDM. Little analysis of these processes exists in the literature, and we leave the detailed study of these channels for future work.

VI. LHC DISCOVERY POTENTIAL

Now that we have discussed the channels in which one might look for a leptonically-decaying Higgs boson at the LHC, let us investigate the prospects for the discovery of such a Higgs boson in the L2HDM, using the combined results from all channels discussed above (excepting the Wh, Zh channels, which we have shown do not contribute significantly to the discovery potential). In particular, we focus on the region of $\sin\alpha - \tan\beta$ parameter space in which η_ℓ is large and η_q, $\eta_V \sim 1$. In this case, the cross sections for processes involving a $h\bar{\ell}\ell$ coupling are substantially increased, while those for processes involving hVV, $h\bar{q}q$, or hgg are only slightly reduced. As before, for

TABLE I. SM production cross sections at the LHC for Wh, Zh associated production, with h decays into muon pair or tau pair. The Higgs mass is taken to be 120 GeV. Also shown are the SM background ZZ, WZ with one Z decays into muons or taus. The numbers are obtained using MADGRAPH [41].

	Signal (fb)	BG (fb)		Signal(fb)	BG(fb)
$Zh(h \to \mu\mu)$	0.113	1156.5	$Zh(h \to \tau\tau)$	32.58	1156.5
$Wh(h \to \mu\mu)$	0.215	1534.3	$Wh(h \to \tau\tau)$	61.85	1534.3

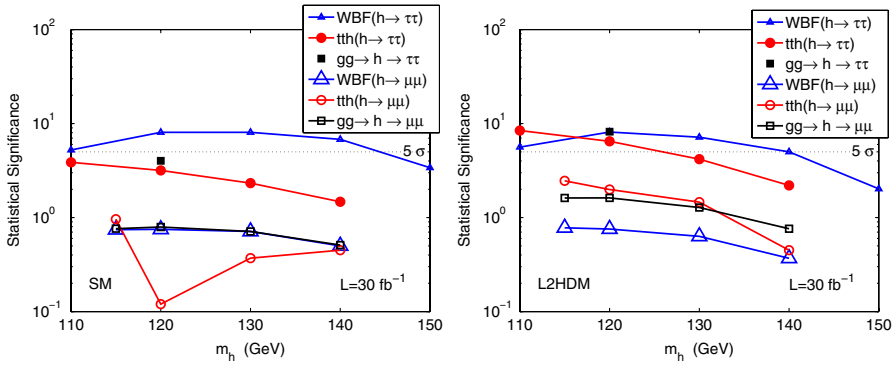

FIG. 9 (color online). Plots of the statistical significances in the leptonic channels discussed in Sec. V for 30 fb^{-1} of integrated luminosity at the LHC. The left-hand panel displays the results for the SM. The right-hand panel displays the results for ($\sin\alpha = 0.55$, $\tan\beta = 3$), in the L2HDM. The standard model results are taken from [1,35,36,39,40]. Note that the $gg \to h \to \tau\tau$ "curve" displayed in each plot consists of a single datum point at $m_h = 120$ GeV. The dip in the SM curve corresponding to the $tth(h \to \mu\mu)$ channel is due to the discrete nature of the Poisson-statistics method used in the analysis [40].

purposes of illustration, we will focus on the benchmark point ($\sin\alpha = 0.55$, $\tan\beta = 3$), which exemplifies this situation nicely. In Fig. 9, we show the effect of the coupling-constant modifications on the discovery potential of a light Higgs boson for this particular benchmark point. In the right-hand panel, the statistical significance associated with each of the relevant leptonic channels discussed in Sec. V is displayed as a function of Higgs mass for our chosen benchmark point in the L2HDM. The SM results for the same processes are shown in the left panel for comparison. The results in each panel correspond to an integrated luminosity of $\mathcal{L} = 30$ fb^{-1}.

It is apparent from Fig. 9 that $qq' \to qq'h(h \to \tau^+\tau^-)$ is one of the most promising detection channels for the chosen benchmark point in the L2HDM, as in the SM. For this particular choice of parameters, $\eta_V \eta_\ell \approx 1$ and $\Gamma_{\rm tot}(h)$ does not deviate drastically from $\Gamma^{\rm SM}_{\rm tot}(h)$ (see Fig. 8), and consequently the overall significance level in this channel is essentially unchanged from its SM value. However, in other regions of parameter space, drastic amplifications can occur:,, for example, the choice ($\sin\alpha = 0.3$, $\tan\beta = 7$) results in a amplification of the statistical significance for the same process by a factor of $\sim$4. It should also be noted that in the ($\sin\alpha = 0.55$, $\tan\beta = 3$) case, the significance levels for both $gg \to h \to \tau\tau$ and $t\bar{t}h(h \to \tau\tau)$ also exceed 5σ. The processes in which the Higgs decays to muons are statistically less significant, but also provide strong evidence at the 3σ level with $\gtrsim 100$ fb^{-1} of integrated luminosity. Indeed, the evidence for such a Higgs boson would be dramatic and unmistakable. Furthermore, once the Higgs is observed in any of the muonic channels, the excellent invariant-mass resolution of the muon pairs can be used to determine the value of m_h with a very high degree of precision.

While the significances in those channels which involve a leptonically-decaying Higgs can potentially be amplified in L2HDM, those in other channels useful for the detection of a SM Higgs may be substantially suppressed. This is illustrated in Fig. 10, which shows the significance of discovery in each individual channel which contributes

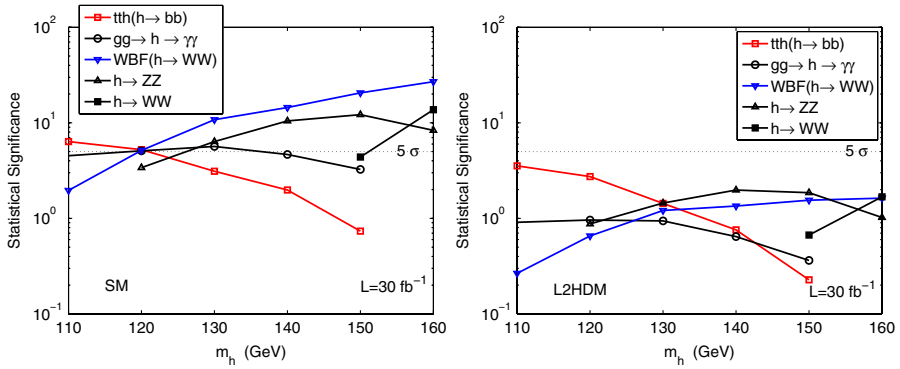

FIG. 10 (color online). The left-hand panel in this plot displays the statistical significances in the nonleptonic channels that contribute significantly to the discovery potential of a light Higgs boson in the SM for 30 fb^{-1} of integrated luminosity at the LHC. The right-hand panel shows the corresponding significances in the L2HDM with ($\sin\alpha = 0.55$, $\tan\beta = 3$). The standard-model results are taken from [5].

meaningfully to the discovery potential of a SM Higgs boson in the low to intermediate-mass region, both in the SM (left-hand panel) and in the L2HDM at the benchmark point ($\sin\alpha = 0.55$, $\tan\beta = 3$) (right-hand panel). In the latter case, there is no single, nonleptonic channel in which evidence for the Higgs boson can be obtained at the 5σ level. To further illustrate the point, in Fig. 11, we display the combined statistical significances for the leptonic channels discussed in Sec. V, as well as the combined significances for all other relevant channels for Higgs discovery, both in the SM and in the L2HDM at the benchmark point ($\sin\alpha = 0.55$, $\tan\beta = 3$). Indeed, for this particular parameter choice, all relevant nonleptonic channels are suppressed relative to their standard model to such an extent that, for most of the $120\ \text{GeV} \lesssim m_h \lesssim 140\ \text{GeV}$ mass window displayed in the plot, their combined significance does not even provide 3σ evidence for—much less a 5σ discovery of—a light Higgs boson. On the other hand, statistical significance for leptonic Higgs decay channels are enhanced, therefore becoming the dominant discovery channels for the light *CP*-even Higgs in the L2HDM model. This clearly illustrates the crucial role leptonic channels can play in the LHC phenomenology of models with extended (and particularly leptophilic) Higgs sectors.

We emphasize that these plots represent the results for a single benchmark point, and one in which the η-factors are not particularly extreme. There exist other points in the parameter space of the model allowed by all constraints for which the deviations of the effective couplings of h to the other fields in the theory are even more severe. As an example, consider the case in which $\sin\alpha = 0.65$ and $\tan\beta = 2.2$, for which $\eta_q = 0.84$, $\eta_\ell = -1.57$, and

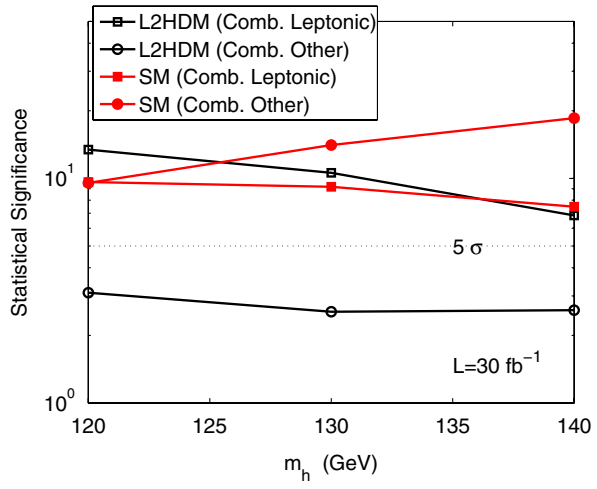

FIG. 11 (color online). The combined statistical significances for the leptonic channels discussed in Sec. V, as well as the combined significances for all other relevant channels for light *CP*-even Higgs discovery in the low to intermediate-mass region, both in the SM and in the L2HDM at the benchmark point ($\sin\alpha = 0.55$, $\tan\beta = 3$). The dotted, horizontal line corresponds to a statistical significance at the 5σ level.

$\eta_{W,Z} = 0.30$. For this choice of parameters, most of the standard Higgs discovery channels—those involving $h \to WW^*$ and $h \to ZZ^*$, as well as all weak-boson-fusion processes not involving direct Higgs decays to leptons—are strongly suppressed; furthermore, other contributing channels such as $gg \to h \to \gamma\gamma$ and $t\bar{t}h(h \to b\bar{b})$ are also moderately suppressed. In such a case, the leptonic channels discussed in Section V—especially ones such as $tth(h \to \tau\tau)$, which do not involve a direct coupling between h and the electroweak gauge bosons—may well constitute the only observable evidence of the Higgs boson, and would thus be crucial for its discovery at the LHC.

VII. CONCLUSION

The phenomenology of a light Higgs boson in two-Higgs-doublet models can differ drastically from that of a SM Higgs. In this work, we have focused on one particularly interesting example: a leptophilic 2HDM, in which different Higgs bosons are responsible for giving masses to the quark and lepton sectors. We have examined the effect of such a modification on the collider phenomenology of a light Higgs boson in a decoupling regime in which the only light scalar is a standard-model-like Higgs boson, and have shown that a number of collider processes involving the direct decay of the Higgs to a pair of charged leptons can play a crucial role in its discovery. In particular, we have shown that there are regions of parameter space in which the Higgs-boson couplings to leptons can be greatly enhanced. This can have a potentially dramatic effect on the Higgs discovery potential, as signals involving direct, leptonic decays of the Higgs can be substantially amplified. At the same time, signals in some (or in some cases, even all) of the other conventional channels useful for the detection of a standard model Higgs boson can suffer a dramatic suppression. Even when coupling modifications are not severe, leptonic decay processes will also play an important rule in differentiating between the Higgs sector of the standard model and that of other, more complicated scenarios.

ACKNOWLEDGMENTS

We would like to thank Keith Dienes, Tao Han, Chung Kao and Lisa Randall for fruitful discussions and correspondence. We would also like to thank the Kavli Institute of Theoretical Physics at Santa Barbara for its hospitality during the completion of this work. This work was supported in part by the Department of Energy under Grant DE-FG02-04ER-41298.

Note added.—After the completion of the work reported in this paper, a number of papers [9,10,44] appeared which discuss the phenomenology of the L2HDM. Ref. [9] gives a brief presentation on the effect of effective-coupling modification in the decoupling regime. Their results agree with ours. Refs. [10,44] focused on the situation in which H, A and $H^\pm$ are light.

[1] S. Asai *et al.*, Eur. Phys. J. C **32**, s19 (2004).
[2] S. Abdullin *et al.*, Eur. Phys. J. C **39**, 41 (2005).
[3] D. L. Rainwater and D. Zeppenfeld, J. High Energy Phys. 12 (1997) 005.
[4] D. L. Rainwater, D. Zeppenfeld, and K. Hagiwara, Phys. Rev. D **59**, 014037 (1998).
[5] ATLAS Collaboration, CERN Report No. CERN-LHCC-99-15, ATLAS Report No. ATLAS-TDR-15.
[6] G. L. Bayatian *et al.* (CMS Collaboration), J. Phys. G **34**, 995 (2007).
[7] N. Arkani-Hamed, A. G. Cohen and H. Georgi, Phys. Lett. B **513**, 232 (2001).
[8] H. E. Haber, M. J. Herrero, H. E. Logan, S. Penaranda, S. Rigolin, and D. Temes, Phys. Rev. D **63**, 055004 (2001); M. S. Carena, H. E. Haber, H. E. Logan, and S. Mrenna, Phys. Rev. D **65**, 055005 (2002); **65**, 099902(E) (2002).
[9] V. Barger, H. E. Logan, and G. Shaughnessy, arXiv:0902.0170.
[10] H. S. Goh, L. J. Hall, and P. Kumar, arXiv:0902.0814.
[11] R. M. Barnett, G. Senjanovic, L. Wolfenstein, and D. Wyler, Phys. Lett. B **136**, 191 (1984).
[12] R. M. Barnett, G. Senjanovic, and D. Wyler, Phys. Rev. D **30**, 1529 (1984).
[13] V. D. Barger, J. L. Hewett, and R. J. N. Phillips, Phys. Rev. D **41**, 3421 (1990).
[14] Y. Grossman, Nucl. Phys. **B426**, 355 (1994).
[15] M. Aoki, S. Kanemura, and O. Seto, Phys. Rev. Lett. **102**, 051805 (2009).
[16] J. F. Gunion and H. E. Haber, Phys. Rev. D **67**, 075019 (2003).
[17] D. Phalen, B. Thomas, and J. D. Wells, Phys. Rev. D **75**, 117702 (2007).
[18] J. F. Gunion, H. E. Haber, G. L. Kane, and S. Dawson, *The Higgs Hunter's Guide* (Addison-Wesley, Redwood City, CA, 1990).
[19] A. G. Akeroyd, A. Arhrib, and E. M. Naimi, Phys. Lett. B **490**, 119 (2000); A. Arhrib, arXiv:hep-ph/0012353; I. F. Ginzburg and I. P. Ivanov, arXiv:hep-ph/0312374.
[20] W. M. Yao *et al.* (Particle Data Group), J. Phys. G **33**, 1 (2006).
[21] W. Grimus and L. Lavoura, Phys. Rev. D **66**, 014016 (2002).
[22] H. E. Haber, G. L. Kane, and T. Sterling, Nucl. Phys. **B161**, 493 (1979).
[23] N. G. Deshpande, P. Lo, J. Trampetic, G. Eilam, and P. Singer, Phys. Rev. Lett. **59**, 183 (1987); S. Bertolini, F. Borzumati, and A. Masiero, Phys. Rev. Lett. **59**, 180 (1987); B. Grinstein and M. B. Wise, Phys. Lett. B **201**, 274 (1988); B. Grinstein, R. P. Springer, and M. B. Wise, Phys. Lett. B **202**, 138 (1988).
[24] W. S. Hou and R. S. Willey, Phys. Lett. B **202**, 591 (1988); T. G. Rizzo, Phys. Rev. D **38**, 820 (1988); J. L. Hewett, S. Nandi, and T. G. Rizzo, Phys. Rev. D **39**, 250 (1989).
[25] B. Grinstein and M. B. Wise, Phys. Lett. B **201**, 274 (1988).
[26] P. J. Franzini, Phys. Rep. **173**, 1 (1989).
[27] W. S. Hou, Phys. Rev. D **48**, 2342 (1993).
[28] A. G. Akeroyd and F. Mahmoudi, J. High Energy Phys. 04 (2009) 121.
[29] M. Krawczyk and D. Temes, Eur. Phys. J. C **44**, 435 (2005).
[30] A. Djouadi, J. Kalinowski, and M. Spira, Comput. Phys. Commun. **108**, 56 (1998).
[31] F. Tarrade (ATLAS Collaboration), ''Tau identification at ATLAS, importance, method and confrontation with Monte Carlo and test beam'', talk given at *Hadron Collider Physics Symposium 2005*, July 2005, Les Diablerets, Switzerland, ATL Report. No. ATL-SLIDE-2006-058;A. F. Saavedra (ATLAS Collaboration), ATL Report No. ATL-PHYS-PROC-2009-007.
[32] V. D. Barger and C. Kao, Phys. Lett. B **424**, 69 (1998); S. Dawson, D. Dicus, and C. Kao, Phys. Lett. B **545**, 132 (2002); S. Dawson, D. Dicus, C. Kao, and R. Malhotra, Phys. Rev. Lett. **92**, 241801 (2004).
[33] A. G. Akeroyd, Phys. Lett. B **377**, 95 (1996); A. G. Akeroyd, J. Phys. G **24**, 1983 (1998).
[34] A. Belyaev, T. Han, and R. Rosenfeld, J. High Energy Phys. 07 (2003) 021.
[35] E. Richter-Was and T. Szymocha, ATL Report No. ATL-PHYS-2004-012.
[36] A. Belyaev and L. Reina, J. High Energy Phys. 08 (2002) 041.
[37] Eilam Gross (ATLAS Collaboration), ''$ttH(H \rightarrow \tau\tau, H \rightarrow bb)$'', talk given at *ATLAS Rome Workshop 2005*, June 2005, Rome, Italy.
[38] T. Plehn and D. L. Rainwater, Phys. Lett. B **520**, 108 (2001).
[39] T. Han and B. McElrath, Phys. Lett. B **528**, 81 (2002).
[40] S. Su and B. Thomas, arXiv:0812.1798.
[41] J. Alwall *et al.*, J. High Energy Phys. 09 (2007) 028.
[42] O. Brein, A. Djouadi, and R. Harlander, Phys. Lett. B **579**, 149 (2004).
[43] S. Frixione, P. Nason, and G. Ridolfi, Nucl. Phys. **B383**, 3 (1992).
[44] M. Aoki, S. Kanemura, K. Tsumura, and K. Yagyu, arXiv:0902.4665.